

Application of chiral resonance Lagrangian theories to the muon $g - 2$

Fred Jegerlehner

fjeger@physik.hu-berlin.de

Work in collaboration with Maurice Benayoun et al

EPJ C 72 (2012) 1848/EPJ C 73 (2013) 2453

Matter to the Deepest Int. Conf. Ustroń, Poland , 2-6 September 2013

Thanks to the Institut Fizyki, Uniwersytet Śląski, Katowice for support

Outline of Talk:

- ❖ Effective field theory: the Resonance Lagrangian Approach, broken HLS
- ❖ A minimal version: VMD + sQED solving the τ vs e^+e^- puzzle
- ❖ Global fit of BHLS parameters and prediction of $F_\pi(s)$
- ❖ SM prediction of a_μ using BHLS predictions for $a_\mu^{\text{LO, had}}$
- ❖ Lessons and Outlook

Effective field theory: the Resonance Lagrangian Approach

- Principles to be included: Chiral Structure of QCD, VMD & electromagnetic gauge invariance.
- ❖ General framework: resonance Lagrangian extension of chiral perturbation theory (CHPT), i.e. implement VMD model with Chiral structure of QCD. Specific version Hidden Local Symmetry (HLS) effective Lagrangian
- ❖ CHPT systematic and unambiguous approach to low energy effective QCD: Spontaneously broken chiral symmetry $SU(3) \otimes SU(3)$ [pseudoscalars as Nambu-Goldstone bosons] plus expansion in low momenta and chiral SB effects [$p \sim m_q$; $q = u, d, s$], limitation: ceases to converge for $E \gtrsim 400 \text{ MeV}$, lacks vector resonances ρ, ω, \dots
- ❖ Vector meson dominance model (effective theory of spin 1 vector resonances ρ, ω, \dots): photon has direct coupling to ρ^0 . In quark model (QCD, SM) photons obviously couple to hadrons via the charged quark

VDM: $\mathcal{L}_{\gamma\rho} = \frac{e}{2g_\rho} \rho_{\mu\nu} F^{\mu\nu}$ or $= -\frac{eM_\rho^2}{g_\rho} \rho_\mu A^\mu$

❖ Resonance Lagrangian approach: can be viewed as an attempt to implement the VMD model in a way which is consistent with the chiral structure of QCD.

Construction of HLS model:

● Like in CHPT the basic fields are the unitary matrix fields $\xi_{L,R} = \exp[\pm i P/f_\pi]$, where $P = P_8 + P_0$ is the $SU(3)$ matrix of pseudoscalar fields, with P_0 and P_8 the basic singlet and octet fields, respectively. The pseudoscalar field matrix P :

$$P_8 = \frac{1}{\sqrt{2}} \begin{pmatrix} \frac{1}{\sqrt{2}}\pi_3 + \frac{1}{\sqrt{6}}\eta_8 + & & \pi^+ & K^+ \\ & \pi^- & & \\ & & -\frac{1}{\sqrt{2}}\pi_3 + \frac{1}{\sqrt{6}}\eta_8 & \\ & & & \end{pmatrix},$$

$$P_0 = \frac{1}{\sqrt{6}} \text{diag}(\eta^0, \eta^0, \eta^0); \quad (\pi_3, \eta_8, \eta_0) \Leftrightarrow (\pi^0, \eta, \eta')$$

● The hidden local symmetry (HLS) ansatz is an extension of the CHPT **non-linear sigma model** to a **non-linear chiral Lagrangian** $[\text{Tr } \partial_\mu \xi^\dagger \partial^\mu \xi]$ based on the symmetry pattern $G_{\text{global}}/H_{\text{local}}$, where $G = SU(3)_L \otimes SU(3)_R$ is the chiral group of QCD and $H = SU(3)_V$ the vector subgroup. The hidden local $SU(3)_V$ requires the spin 1 vector meson fields, represented by the $SU(3)$ matrix field V_μ , to be gauge fields. The needed covariant derivative reads $D_\mu = \partial_\mu - i g V_\mu$, allows to include the couplings to the electroweak gauge fields A_μ , Z_μ and W_μ^\pm . The vector field matrix is given by :

$$V = \frac{1}{\sqrt{2}} \begin{pmatrix} (\rho^I + \omega^I)/\sqrt{2} & \rho^+ & K^{*+} \\ \rho^- & (-\rho^I + \omega^I)/\sqrt{2} & K^{*0} \\ K^{*-} & \bar{K}^{*0} & \phi^I \end{pmatrix}$$

The unbroken HLS Lagrangian is then given by

$$\mathcal{L}_{\text{HLS}} = \mathcal{L}_A + \mathcal{L}_V ; \quad \mathcal{L}_{A/V} = -\frac{f_\pi^2}{4} \text{Tr} [L \pm R]^2$$

where $L = [D_\mu \xi_L] \xi_L^+$ and $R = [D_\mu \xi_R] \xi_R^+$.

The covariant derivatives are given by :

$$\begin{cases} D_\mu \xi_L = \partial_\mu \xi_L - igV_\mu \xi_L + i\xi_L \mathcal{L}_\mu \\ D_\mu \xi_R = \partial_\mu \xi_R - igV_\mu \xi_R + i\xi_R \mathcal{R}_\mu \end{cases}$$

with :

$$\begin{cases} \mathcal{L}_\mu = eQA_\mu + \frac{g_2}{\cos \theta_W} (T_z - \sin^2 \theta_W) Z_\mu + \frac{g_2}{\sqrt{2}} (W_\mu^+ T_+ + W_\mu^- T_-) \\ \mathcal{R}_\mu = eQA_\mu - \frac{g_2}{\cos \theta_W} \sin^2 \theta_W Z_\mu \end{cases}$$

- ❖ In fact the global chiral symmetry G_{global} is well known not to be realized as an exact symmetry in nature which implies that the ideal HLS symmetry evidently is not a symmetry of nature either.
- ❖ It evidently has to be broken appropriately in order to provide a realistic low energy effective theory mimicking low energy effective QCD. Corresponding to the strength of the breaking, usually, this has been done in two steps, breaking of $SU(3)$ in a first step and breaking $SU(2)$ isospin in a second step.
- ❖ Unlike in CHPT (perturbed non-linear σ -model) where one is performing a systematic low energy expansion, expanding in low momenta and the quark masses, here we introduce symmetry breaking as phenomenological parameters to be fixed from appropriate data, since a systematic low energy expansion à la CHPT ceases to converge at energies above about 400 MeV, while we attempt to model phenomenology up to including the ϕ resonance.

The broken HLS Lagrangian (BHLS) is then given by

$$\mathcal{L}_{\text{BHLS}} = \mathcal{L}'_A + \mathcal{L}'_V + \mathcal{L}'_{\text{tHooft}} ; \quad \mathcal{L}'_{A/V} = -\frac{f_\pi^2}{4} \text{Tr} \{ [L \pm R] X_{A/V} \}^2$$

with 6 phenomenological chiral SB parameters. SB pattern:

$$X_I = \text{diag}(q_I, y_I, z_I) ; \quad |q_I - 1|, |y_I - 1| \ll |z_I - 1| ; \quad I = V, A .$$

Anomalous sector as well: simplest Wess-Zumino-Witten Lagrangian

$$\mathcal{L}_{\text{WZW}} = \frac{\alpha}{\pi} \frac{N_c}{12F_\pi} \left(\pi^0 + \frac{1}{\sqrt{3}} \eta_8 + 2 \sqrt{\frac{2}{3}} \eta_0 \right) \tilde{F}_{\mu\nu} F^{\mu\nu} ,$$

which is reproducing the ABJ anomaly and is responsible for $\pi^0 \rightarrow \gamma\gamma$ etc.

A minimal version: VMD + sQED solving the τ vs e^+e^- puzzle

Effective Lagrangian $\mathcal{L} = \mathcal{L}_{\gamma\rho} + \mathcal{L}_{\pi}$

$$\begin{aligned}\mathcal{L}_{\pi} &= D_{\mu}\pi^{+}D^{+\mu}\pi^{-} - m_{\pi}^2\pi^{+}\pi^{-} ; \quad D_{\mu} = \partial_{\mu} - ieA_{\mu} - ig_{\rho\pi\pi}\rho_{\mu} \\ \mathcal{L}_{\gamma\rho} &= -\frac{1}{4}F_{\mu\nu}F^{\mu\nu} - \frac{1}{4}\rho_{\mu\nu}\rho^{\mu\nu} + \frac{M_{\rho}^2}{2}\rho_{\mu}\rho^{\mu} + \frac{e}{2g_{\rho}}\rho_{\mu\nu}F^{\mu\nu}\end{aligned}$$

Self-energies: pion loops to photon-rho vacuum polarization

$$\begin{aligned}
 -i \Pi_{\gamma\gamma}^{\mu\nu}(\pi)(q) &= \text{diagram 1} + \text{diagram 2} \\
 -i \Pi_{\gamma\rho}^{\mu\nu}(\pi)(q) &= \text{diagram 3} + \text{diagram 4} \\
 -i \Pi_{\rho\rho}^{\mu\nu}(\pi)(q) &= \text{diagram 5} + \text{diagram 6}
 \end{aligned}$$

The diagrams represent one-loop self-energy corrections to the photon and rho meson propagators. Diagram 1 shows a photon loop (dashed blue circle) on a photon line (red wavy). Diagram 2 shows a pion loop (dashed blue circle) on a photon line. Diagram 3 shows a pion loop on a photon line with a rho meson line (red double line) attached to the loop. Diagram 4 shows a pion loop on a rho meson line with a photon line attached to the loop. Diagram 5 shows a pion loop on a rho meson line. Diagram 6 shows a pion loop on a rho meson line with a rho meson line attached to the loop.

Irreducible self-energy contribution at one-loop

bare $\gamma - \rho$ transverse self-energy functions

$$\Pi_{\gamma\gamma} = \frac{e^2}{48\pi^2} f(q^2), \quad \Pi_{\gamma\rho} = \frac{eg_{\rho\pi\pi}}{48\pi^2} f(q^2) \quad \text{and} \quad \Pi_{\rho\rho} = \frac{g_{\rho\pi\pi}^2}{48\pi^2} f(q^2),$$

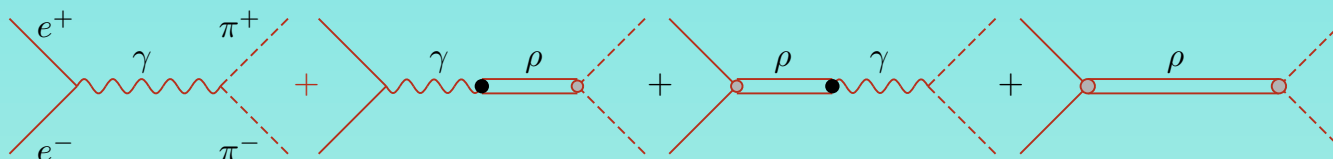
$$\begin{aligned}
-i \Pi_{\gamma\gamma}^{\mu\nu}(\pi)(q) &= \text{[Diagram: wavy line, dashed circle, wavy line]} + \text{[Diagram: wavy line, dashed circle, wavy line]} . \\
-i \Pi_{\gamma\rho}^{\mu\nu}(\pi)(q) &= \text{[Diagram: wavy line, circle, double red line]} . \\
-i \Pi_{\rho\rho}^{\mu\nu}(\pi)(q) &= \text{[Diagram: double red line, dashed circle, double red line]} + \text{[Diagram: double red line, dashed circle, double red line]} .
\end{aligned}$$

Previous calculations, consider mixing term to be constant

The $e^+e^- \rightarrow \pi^+\pi^-$ matrix element in sQED is given by

$$\mathcal{M} = -i e^2 \bar{v} \gamma^\mu u (p_1 - p_2)_\mu F_\pi(q^2)$$

with $F_\pi(q^2) = 1$. In our extended VMD model we have the four terms



Diagrams contributing to the process $e^+e^- \rightarrow \pi^+\pi^-$.

$$F_\pi(s) \propto e^2 D_{\gamma\gamma} + e g_{\rho\pi\pi} D_{\gamma\rho} - g_{\rho ee} e D_{\rho\gamma} - g_{\rho ee} g_{\rho\pi\pi} D_{\rho\rho},$$

Properly normalized (VP subtraction: $e^2(s) \rightarrow e^2$):

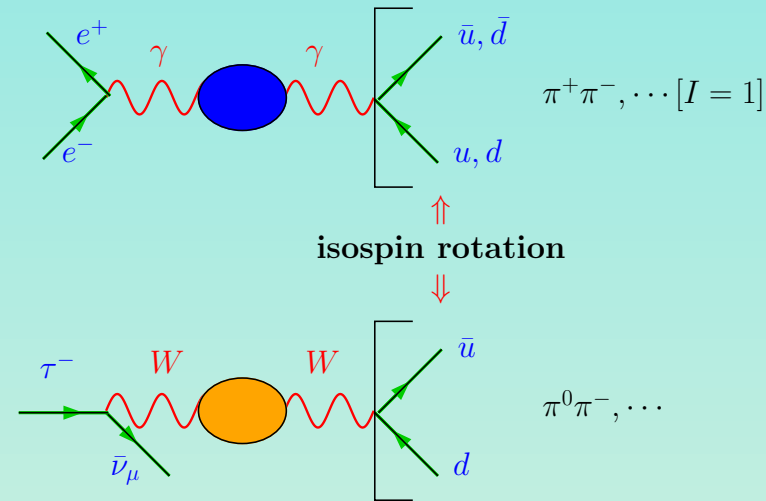
$$F_\pi(s) = \left[e^2 D_{\gamma\gamma} + e (g_{\rho\pi\pi} - g_{\rho ee}) D_{\gamma\rho} - g_{\rho ee} g_{\rho\pi\pi} D_{\rho\rho} \right] / \left[e^2 D_{\gamma\gamma} \right]$$

Typical couplings

$$g_{\rho\pi\pi \text{ bare}} = 5.8935, \quad g_{\rho\pi\pi \text{ ren}} = 6.1559, \quad g_{\rho ee} = 0.018149, \quad x = g_{\rho\pi\pi}/g_\rho = 1.15128.$$

$$g_{\rho\pi\pi} = \sqrt{48 \pi \Gamma_\rho / (\beta_\rho^3 M_\rho)}; \quad g_{\rho ee} = \sqrt{12 \pi \Gamma_{\rho ee} / M_\rho}$$

- ❖ Good old idea: use isospin symmetry to include existing high quality τ -data (including isospin corrections)

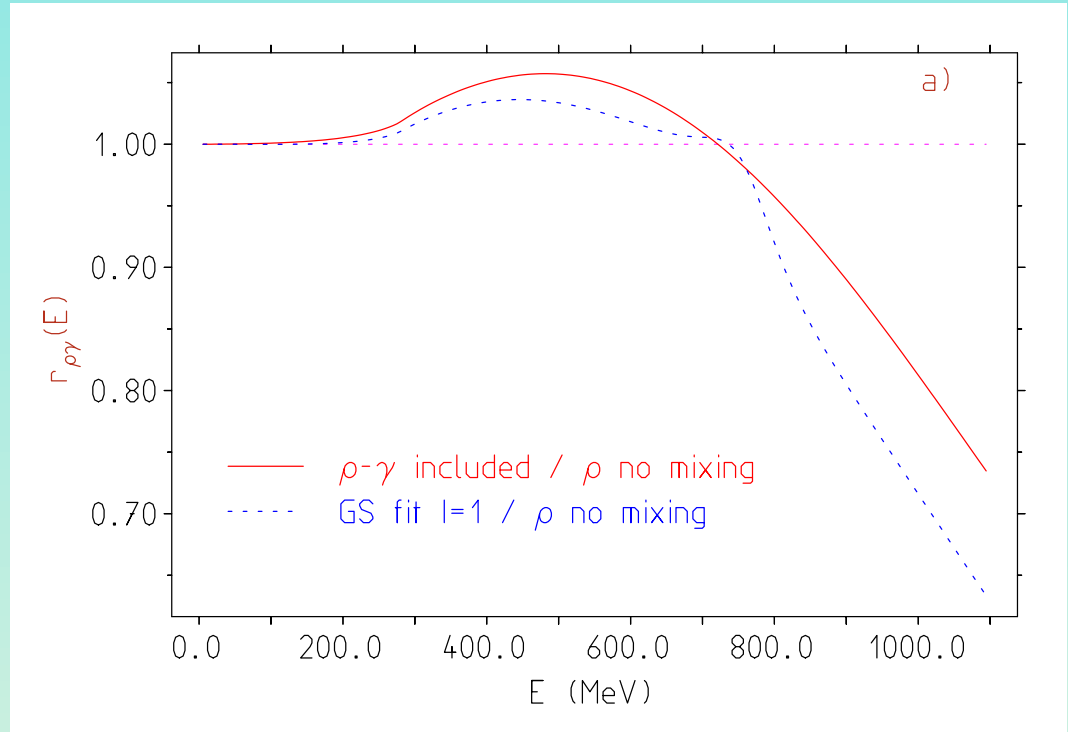


Corrected data: large discrepancy [$\sim 10\%$] persists! τ vs. e^+e^- problem! [manifest since 2002]

Recent: τ (charged channel) vs. e^+e^- (neutral channel) puzzle resolved
 F.J.& R. Szafron, $\rho - \gamma$ interference
 (absent in charged channel):

$$-i \Pi_{\gamma\rho}^{\mu\nu}(\pi)(q) = \text{diagram 1} + \text{diagram 2}$$

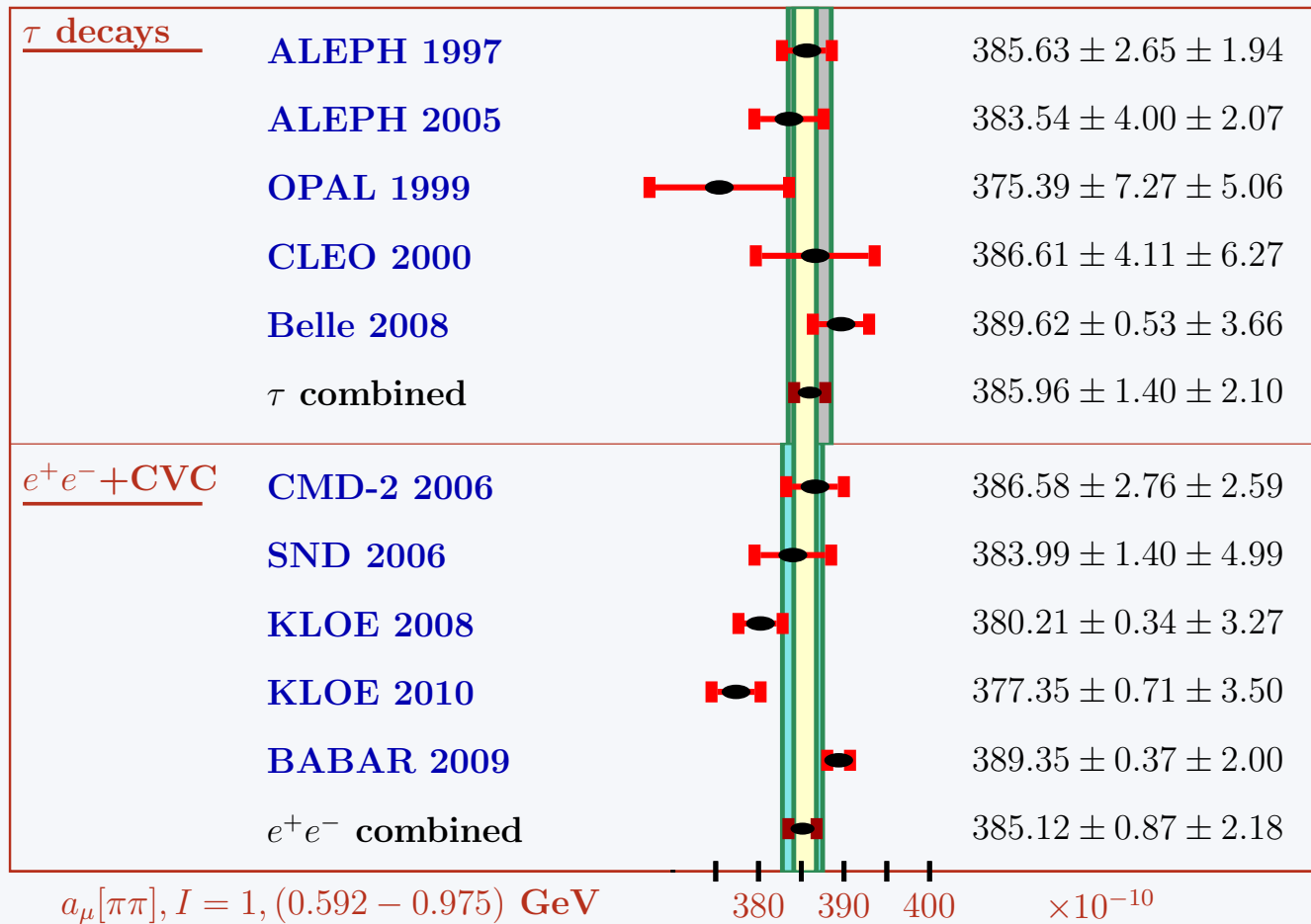
$$v_0(s) = r_{\rho\gamma}(s) R_{\text{IB}}(s) v_-(s)$$



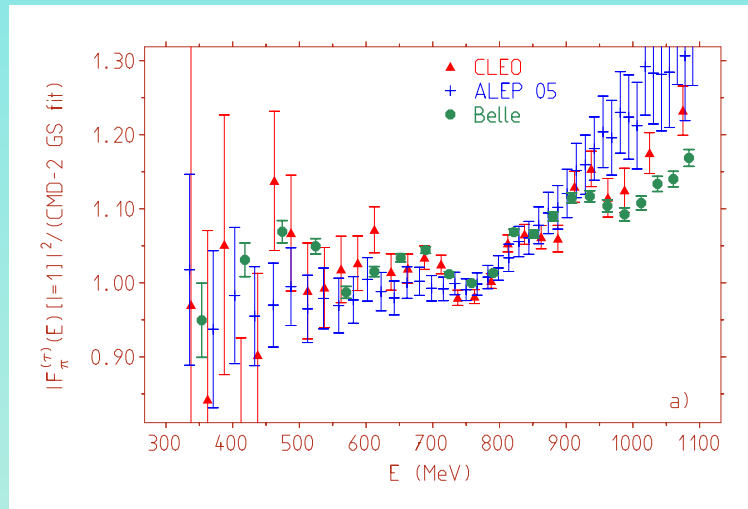
- τ data require to be corrected for missing $\rho - \gamma$ mixing!
- results obtained from e^+e^- data is what goes into a_μ



$l=1$ part of $a_\mu^{\text{had}}[\pi\pi]$

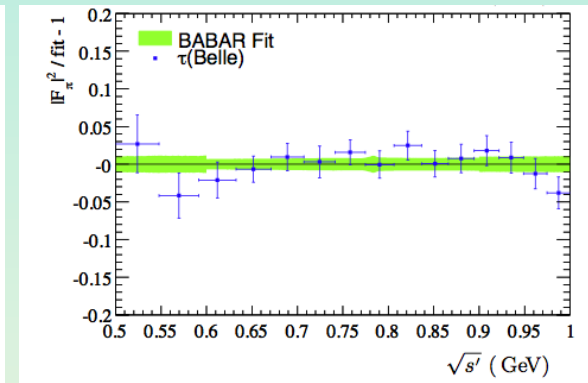
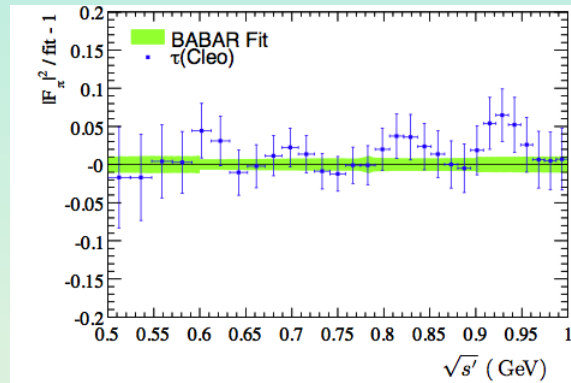
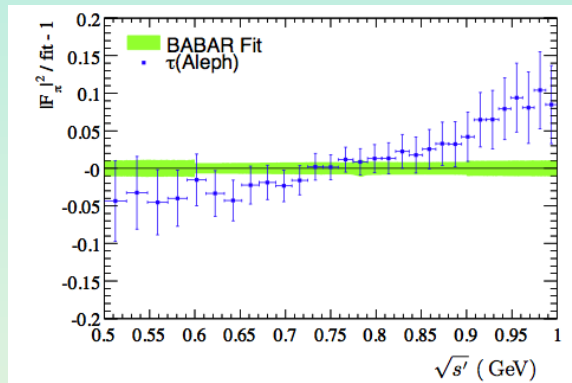


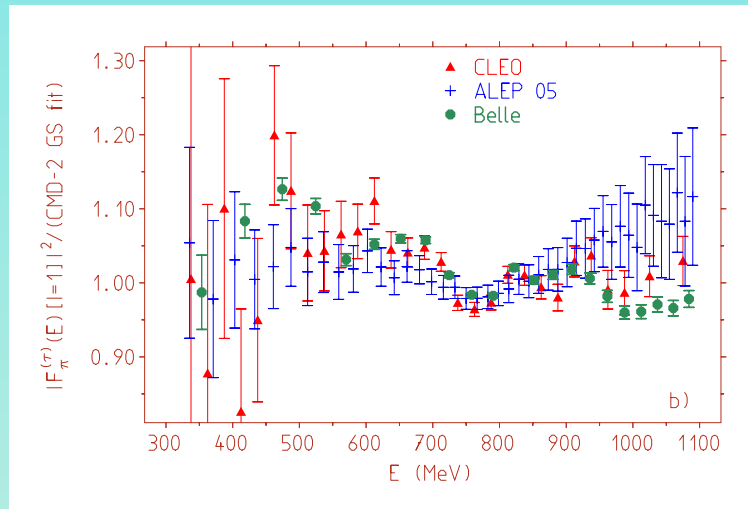
$I=1$ part of $a_\mu^{\text{had}}[\pi\pi]$



$|F_\pi(E)|^2$ in units of $e^+e^- I=1$ (CMD-2 GS fit)

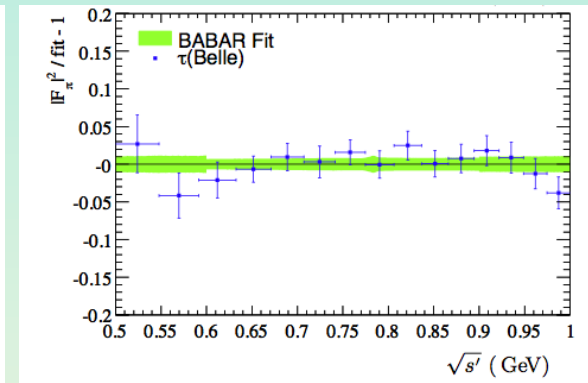
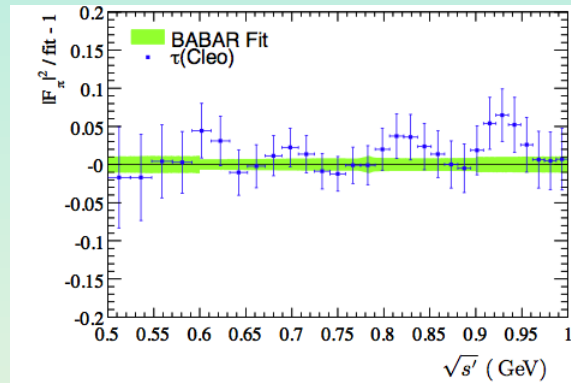
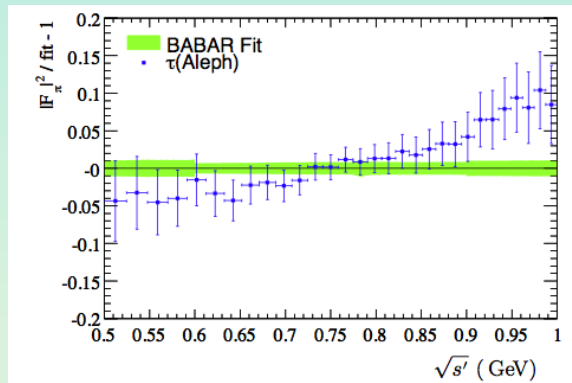
Best “proof”:



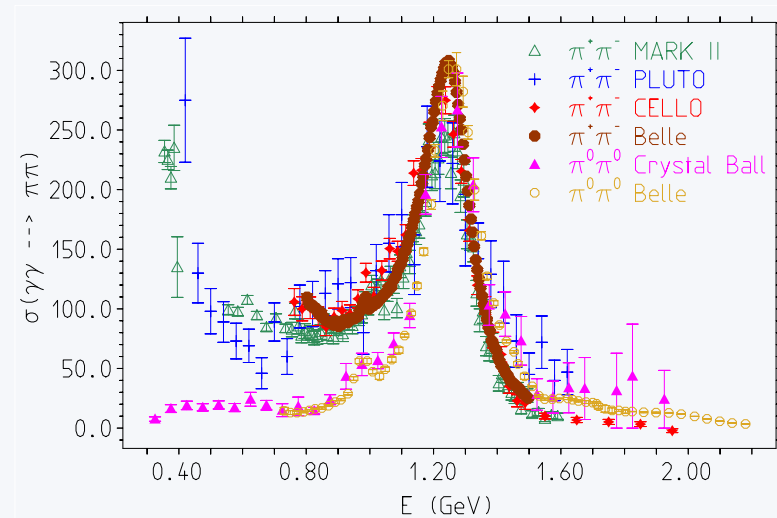


$|F_{\pi}(E)|^2$ in units of $e^+e^- |l=1$ (CMD-2 GS fit)

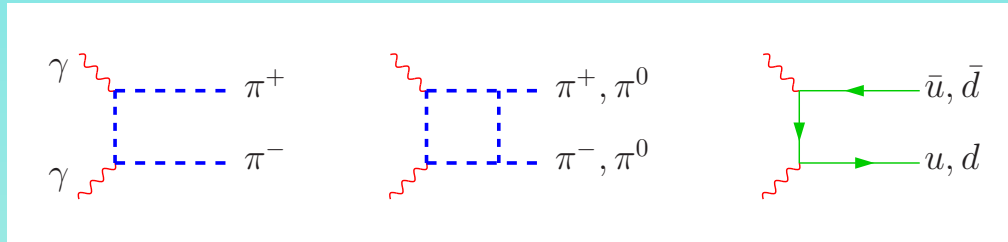
Best “proof”:



Is our model viable?



How photons couple to pions? This is obviously probed in reactions like $\gamma\gamma \rightarrow \pi^+\pi^-, \pi^0\pi^0$. Data infer that below about 1 GeV photons couple to pions as point-like objects (i.e. to the charged ones overwhelmingly), at higher energies the photons see the quarks exclusively and form the prominent tensor resonance $f_2(1270)$. The $\pi^0\pi^0$ cross section in this figure is enhanced by the isospin symmetry factor 2, by which it is reduced in reality.



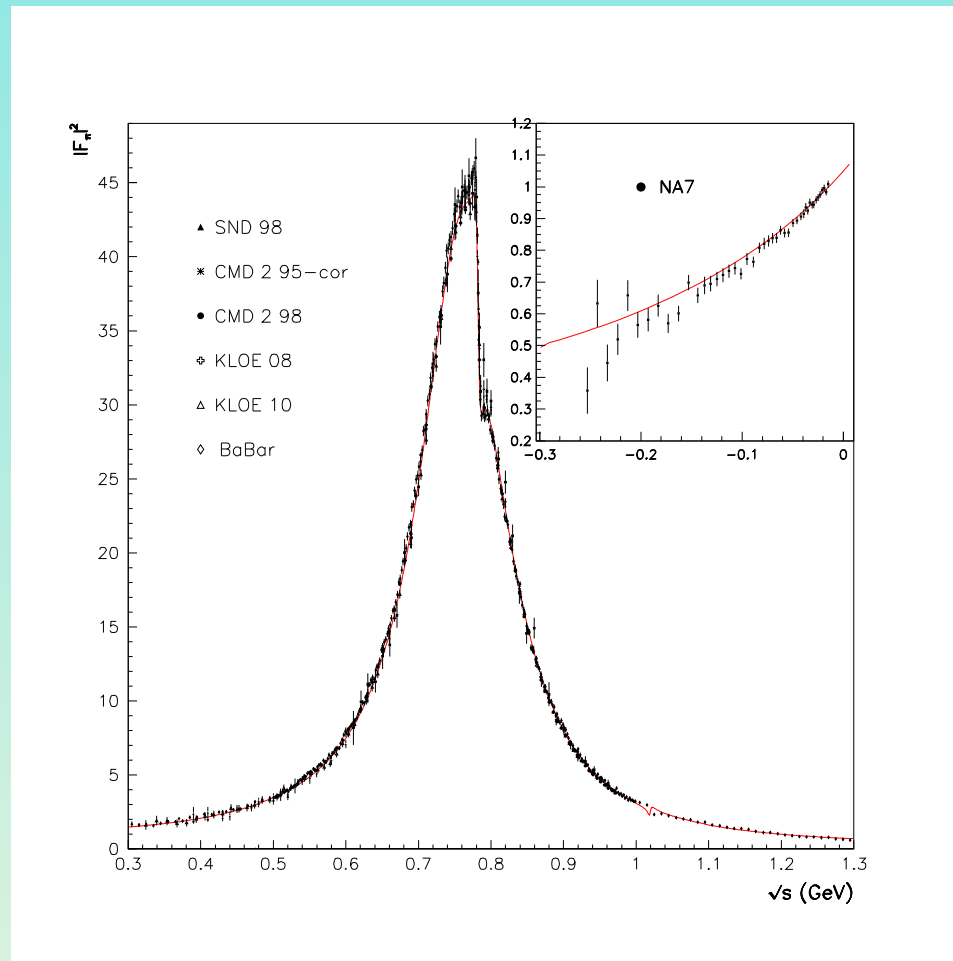
Di-pion production in $\gamma\gamma$ fusion. At low energy we have direct $\pi^+\pi^-$ production and by strong rescattering $\pi^+\pi^- \rightarrow \pi^0\pi^0$, however with very much suppressed rate.

Above about 1 GeV, resolved $q\bar{q}$ couplings seen.

Strong tensor meson resonance in $\pi\pi$ channel $f_2(1270)$ with photons directly probe the quarks!

- Photons seem to see pions below 1 GeV
- Photons definitely look at the quarks in $f_2(1270)$ resonance region
- We apply the sQED model up to 0.975 GeV (relevant for a_μ). This should be pretty save (still we assume a 10% model uncertainty)
- Switching off the electromagnetic interaction of pions, is definitely not a realistic approximation in trying to describe what data we see in $e^+e^- \rightarrow \pi^+\pi^-$

Global fit of BHLS parameters and prediction of $F_\pi(s)$



Fit τ + IB from PDG vs $\pi^+\pi^-$

Data below $E_0 = 1.05 \text{ GeV}$ (just above the ϕ) constrain effective Lagrangian couplings, using 45 different data sets (6 annihilation channels and 10 partial width decays).

□ Effective theory predicts cross sections:

$$\pi^+\pi^-, \pi^0\gamma, \eta\gamma, \eta'\gamma, \pi^0\pi^+\pi^-, K^+K^-, K^0\bar{K}^0 \quad (83.4\%),$$

● Missing part:

$$4\pi, 5\pi, 6\pi, \eta\pi\pi, \omega\pi \text{ and regime } E > E_0$$

evaluated using data directly and pQCD for perturbative region and tail

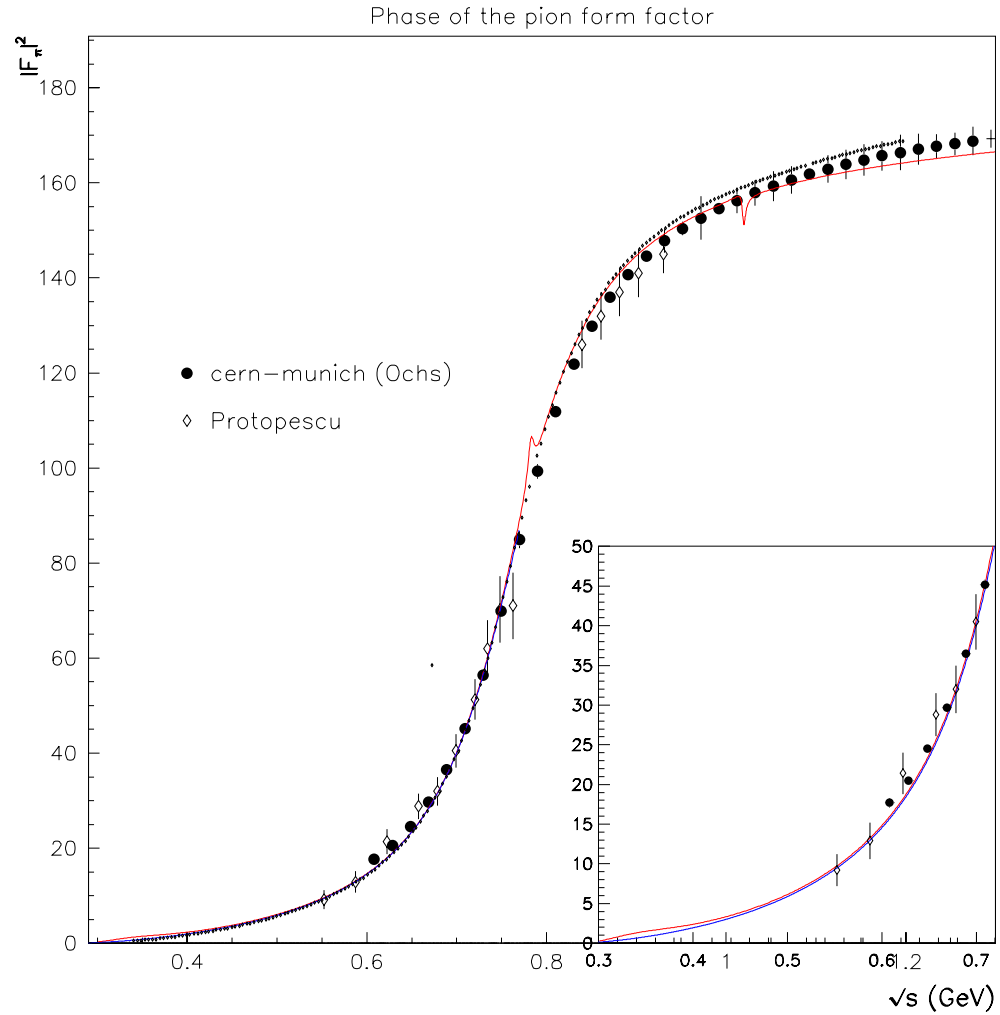
● Including **self-energy effects** is mandatory ($\gamma\rho$ -mixing, $\rho\omega$ -mixing ..., decays with proper phase space, energy dependent width etc)

● Method works in reducing uncertainties by using **indirect constraints**

● Able to reveal inconsistencies in data. In our case in region $[1.00, 1.05] \text{ GeV}$ tension between KK and 3π data sets. All data: Solution A 71.2% CL; excluding 3π above 1 GeV: Solution B 97.0% CL. Conflict in data?, model?

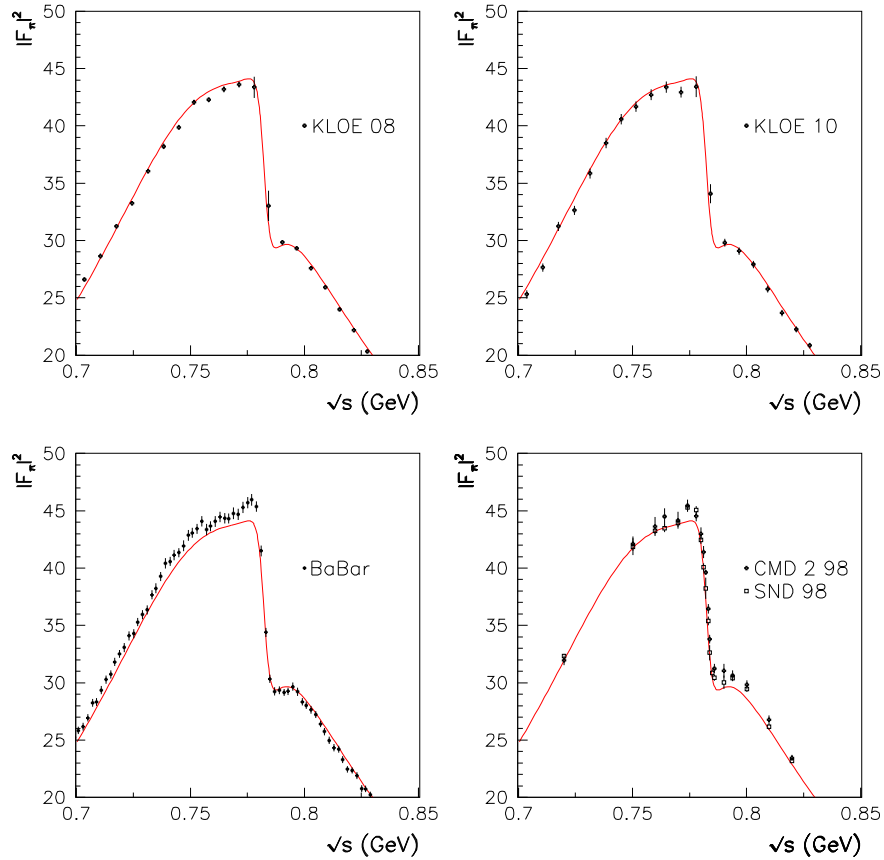
Main goal:

- **Single out** representative effective resonance Lagrangian by global fit is expected to help in improving EFT calculations of **hadronic light-by-light scattering** (such concept so far missing)
- could help improving uncertainty on hadronic VP
- **new muon g-2 experiment** to start at Fermilab in about 2-3 years: reducing experimental error by **factor 4**
- requires same improvement of hadronic VP and LbL then **$3\sigma \Rightarrow 9\sigma$**

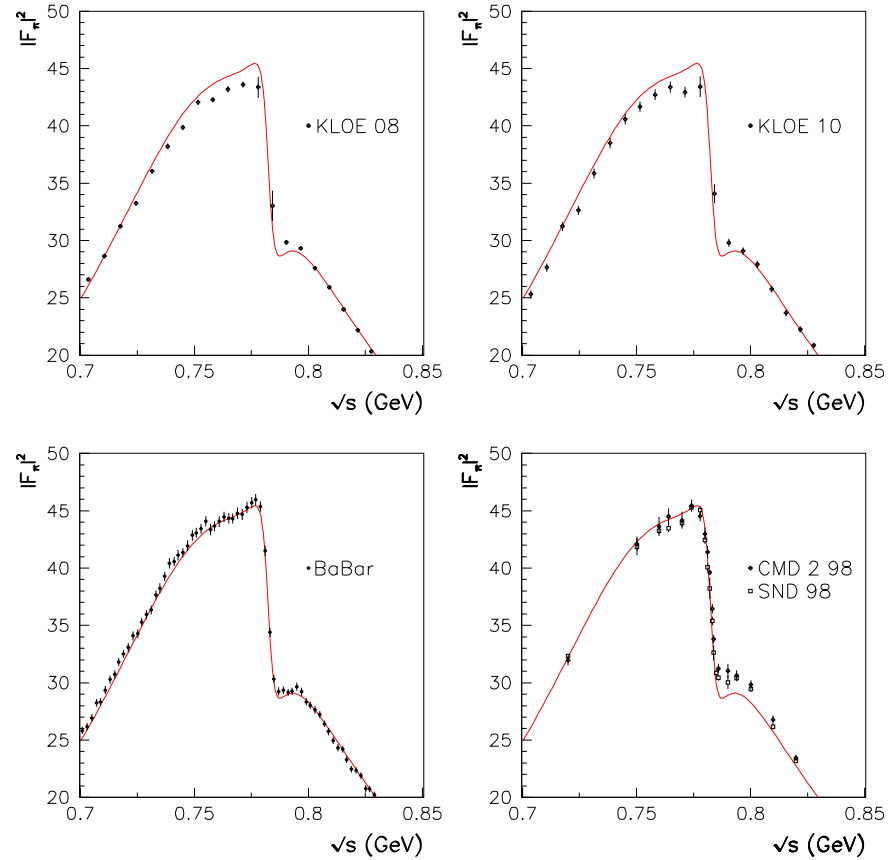


The $\pi\pi$ scattering phase of our HLS prediction

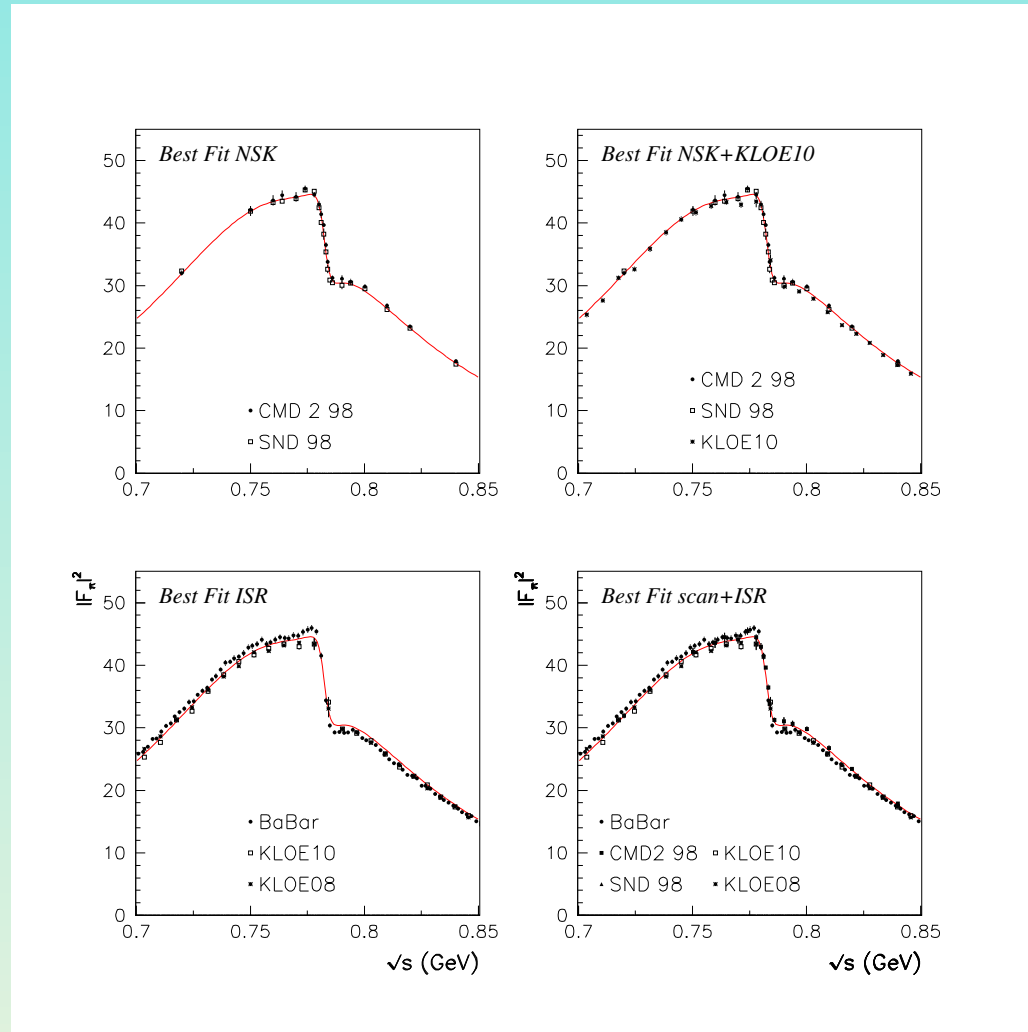
Fit of τ +PDG vs $\pi^+\pi^-$ -data



Fit of BaBar vs other $\pi^+\pi^-$ -data



Best fits of τ + PDG + selected $\pi^+\pi^-$ -data



SM prediction of a_μ using BHLS predictions for $a_\mu^{\text{LO, had}}$

$10^{10} a_\mu$	Values (incl. τ)		Values (excl. τ)	
	no ISR	with ISR [new]	scan + ISR	scan only
LO hadronic	684.46 ± 4.60	685.81 ± 4.23	686.73 ± 4.32	682.31 ± 4.99
HO hadronic	-9.97 ± 0.09			
LBL	10.5 ± 2.6			
QED	$11\,658\,471.8851 \pm 0.0036$			
EW	$15.40 \pm 0.10_{\text{had}} \pm 0.03_{\text{Higgs, top, 3-loop}}$			
Theor.	$11\,659\,172.22 \pm 5.21$	$11\,659\,173.54 \pm 4.89$	$11\,659\,174.46 \pm 4.97$	$11\,659\,170.04 \pm 5.55$
Exper.	$11\,659\,209.1 \pm 6.3$			
Δa_μ	36.91 ± 8.18	35.56 ± 7.98	34.64 ± 8.02	38.86 ± 8.40
S.D. ($n\sigma$)	4.51σ	4.46σ	4.32σ	4.63σ

The various contributions to $10^{10} a_\mu$. $\Delta a_\mu = (a_\mu)_{\text{exp}} - (a_\mu)_{\text{the}}$ is given in units of 10^{-10}

Hadronic VP contributions to $10^{10}a_\mu$ with FSR corrections included.

Final State	Range (GeV)	Contribution (incl. τ)		Contribution (excl. τ)	
		Solution A	Solution B	Solution A	Solution B
$e^+e^- \rightarrow$ hadrons	threshold \rightarrow 1.05	572.82[1.90]	574.76[2.10]	569.86[2.15]	571.40[2.27]
missing channels	threshold \rightarrow 1.05	1.55(0.40)(0.40)[0.57]			
J/ψ		8.51(0.40)(0.38)[0.55]			
Υ		0.10(0.00)(0.10)[0.10]			
hadronic	(1.05, 2.00)	60.76(0.22)(3.93)[3.94]			
hadronic	(2.00, 3.10)	21.63(0.12)(0.92)[0.93]			
hadronic	(3.10, 3.60)	3.77(0.03)(0.10)[0.10]			
hadronic	(3.60, 5.20)	7.64(0.04)(0.05)[0.06]			
pQCD	(5.20, 9.46)	6.19(0.00)(0.00)[0.00]			
hadronic	(9.46, 13.00)	1.28(0.01)(0.07)[0.07]			
pQCD	(13.00, ∞)	1.53(0.00)(0.00)[0.00]			
Total	1.05 \rightarrow ∞ + missing channels	$112.96 \pm 4.13_{tot}$			
Total Model	threshold \rightarrow ∞	685.78 ± 4.55	687.72 ± 4.63	682.82 ± 4.66	684.36 ± 4.71

Our favored evaluation is : $a_{\mu}^{\text{LO had}} = (682.11 \pm 4.52) \times 10^{-10}$

$$a_{\mu}^{\text{the}} = (11659169.80 \pm 5.22) \times 10^{-10},$$

$$\Delta a_{\mu} = a_{\mu}^{\text{exp}} - a_{\mu}^{\text{the}} = (39.21 \pm 5.22_{\text{the}} \pm 6.3_{\text{exp}}) \times 10^{-10},$$

The associated fit probability is **94%** and the significance for Δa_{μ} is **4.8 σ**

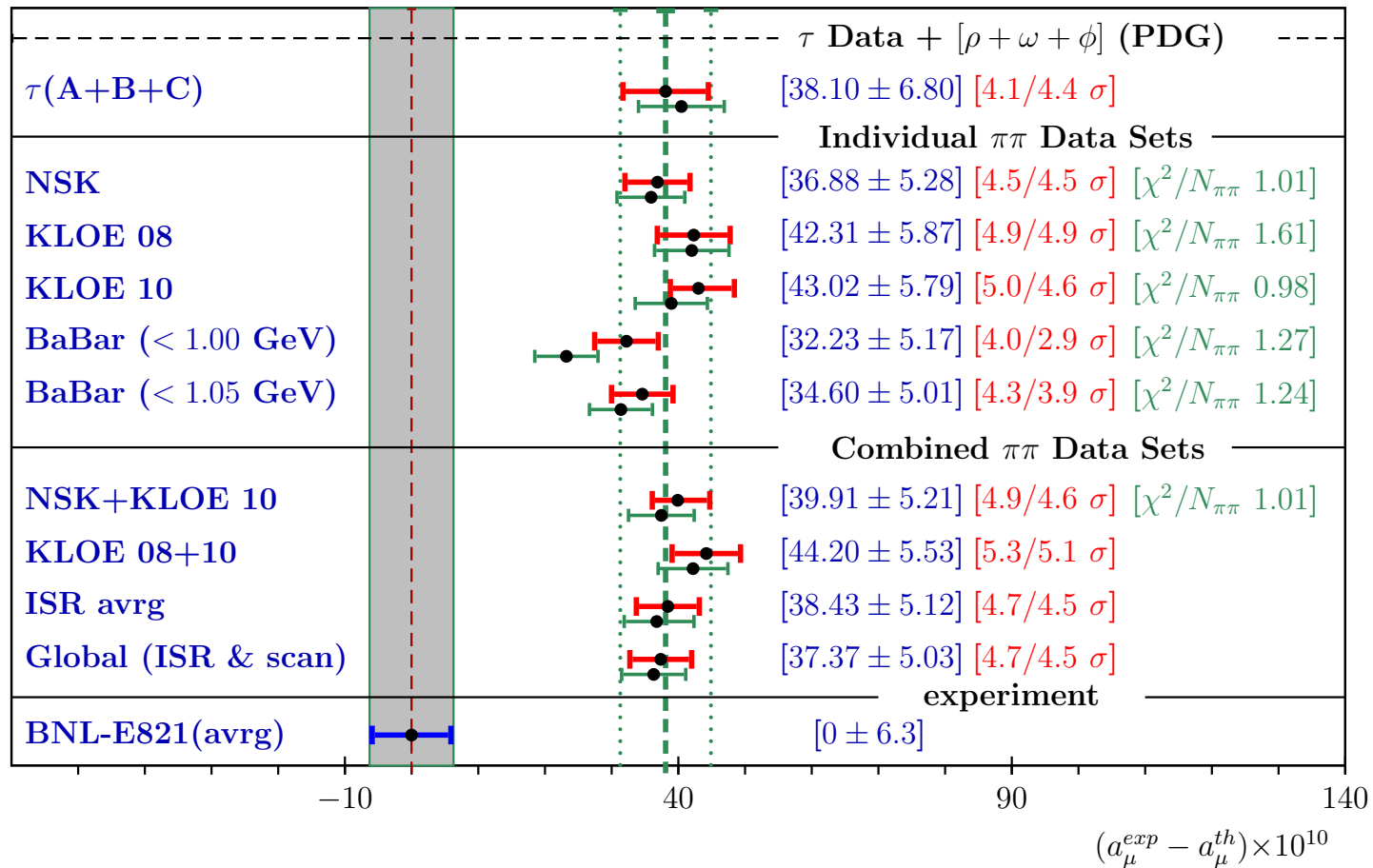
Including all data: $a_{\mu}^{\text{LO had}} = (685.81 \pm 4.23) \times 10^{-10}$

$$a_{\mu}^{\text{the}} = (11659173.50 \pm 4.97) \times 10^{-10},$$

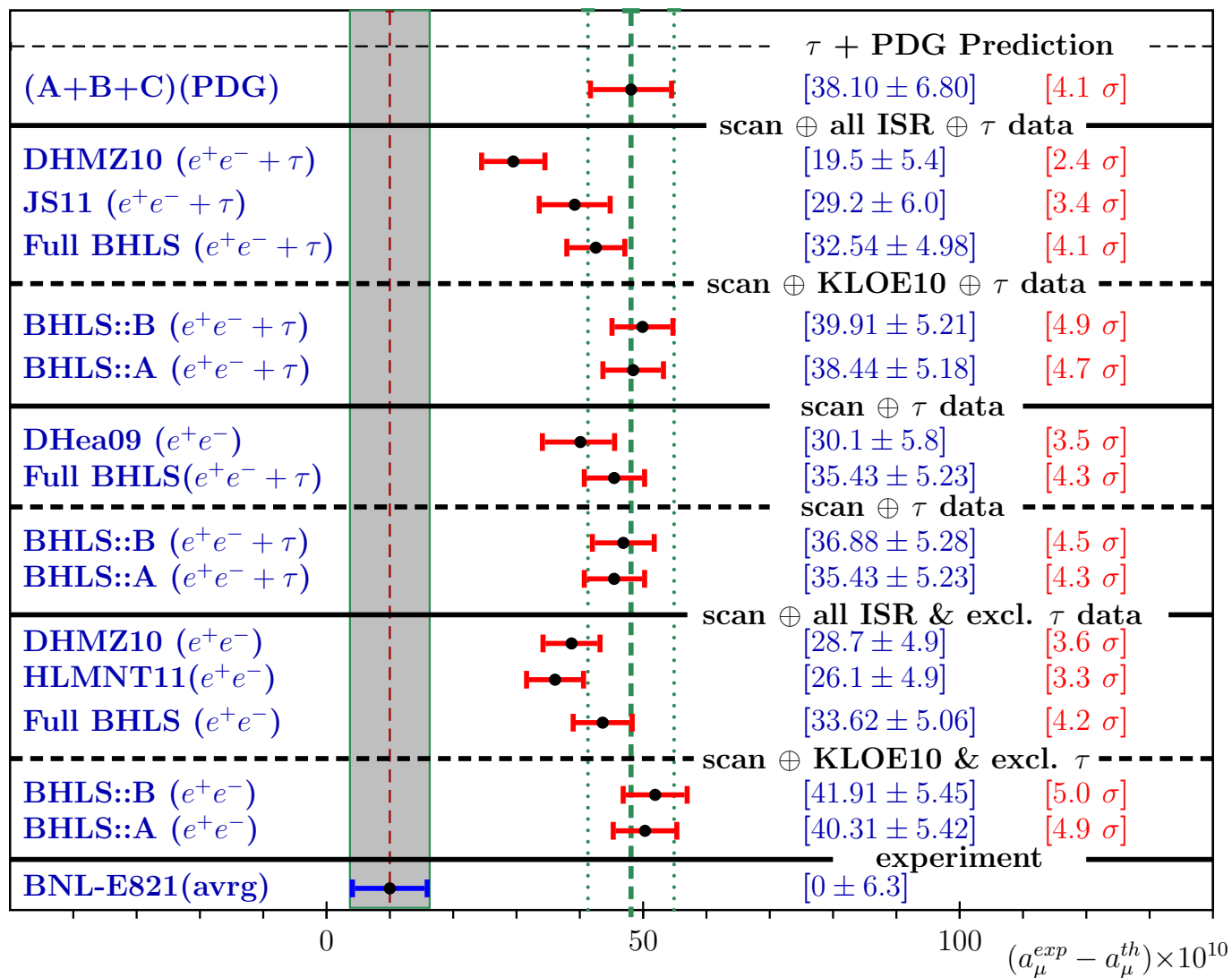
$$\Delta a_{\mu} = a_{\mu}^{\text{exp}} - a_{\mu}^{\text{the}} = (35.51 \pm 4.97_{\text{the}} \pm 6.3_{\text{exp}}) \times 10^{-10},$$

The associated fit probability is **76%** and the significance for Δa_{μ} is **4.4 σ**

(requires reweighting of $e^+e^- \rightarrow \pi^+\pi^-\pi^0$ in vicinity of the ϕ as well as KLOE08 and BaBar $e^+e^- \rightarrow \pi^+\pi^-$)



Comparison of various Fits



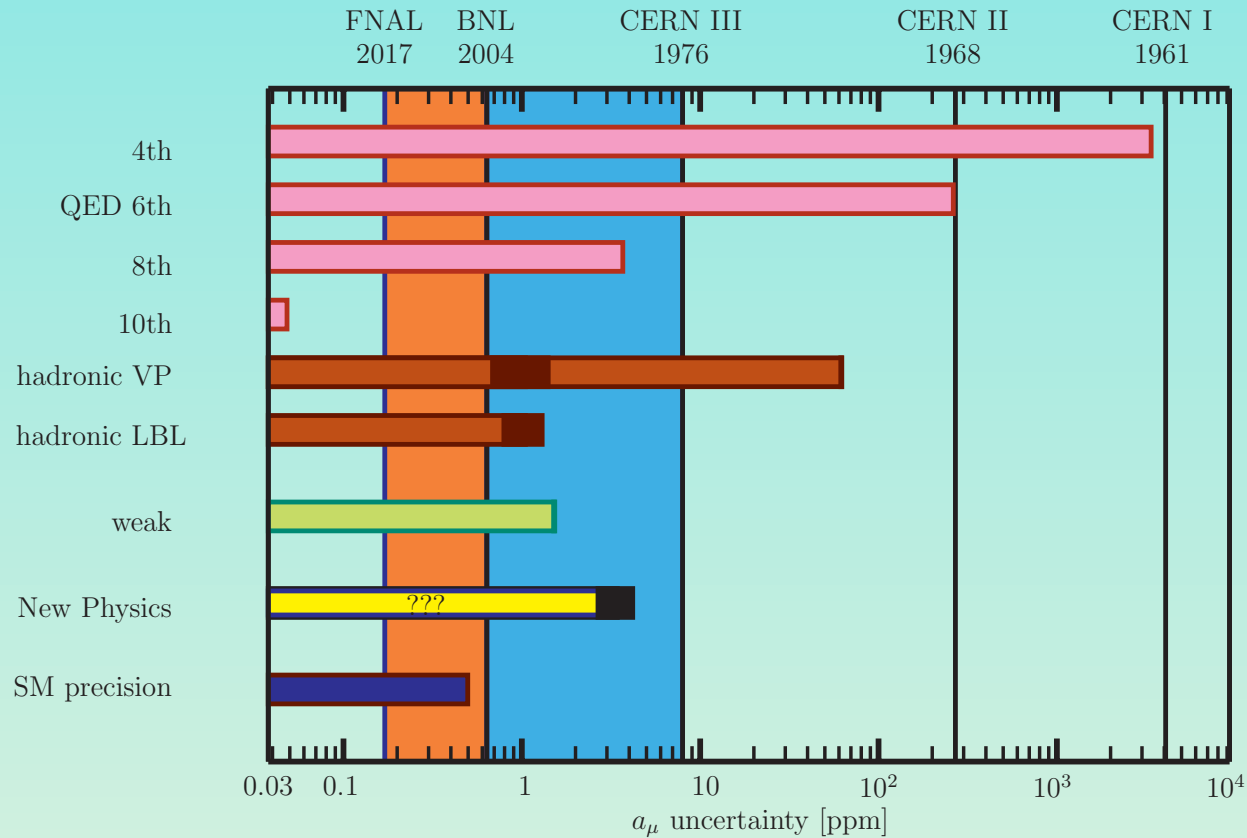
Comparison with other Results

Lessons and Outlook

- Effective field theory is the only way to understand relationships between different channels, like e^+e^- -annihilation cross-sections and τ -decay spectra
- Global fit strategies allow to single out variants of effective resonance Lagrangian models
- Models for individual channels can parametrize data, but do not allow to understand them and their relation to other channels
- We get perfect fits for $|F_\pi(s)|^2$ up to just above the ϕ without higher ρ 's ρ', ρ'' , which seem to be mandatory in Gounaris-Sakurai type fits.
- τ data in our approach play special role, much simpler than e^+e^- with its intricate $\gamma - \rho^0 - \omega - \phi$ mixing.
- $\pi^+\pi^-$ cross-section from τ spectra plus isospin breaking encoded in $\rho \rightarrow e^+e^-$ [main issue in τ vs e^+e^-], $\omega \rightarrow \pi^+\pi^-$ etc

- RLA type analyses provide analytic shapes for amplitudes, and such “physical shape information” is favorable over ad hoc data interpolations (the simplest being the trapezoidal rule, which is known to be problematic when data are sparse or strongly energy dependent).
- Limitations: large couplings, higher order effects?, range of validity, e.g. point-like pions (sQED) etc.
- Our analysis is a starting point to be confronted with other RLA versions and implementations including higher order effects.
- Good starting point for reevaluation of hadronic light-by-light contribution to muon $g - 2$. So far no “globally verified” framework applied.
- Last but not least: there is no τ vs e^+e^- problem

And here we are:



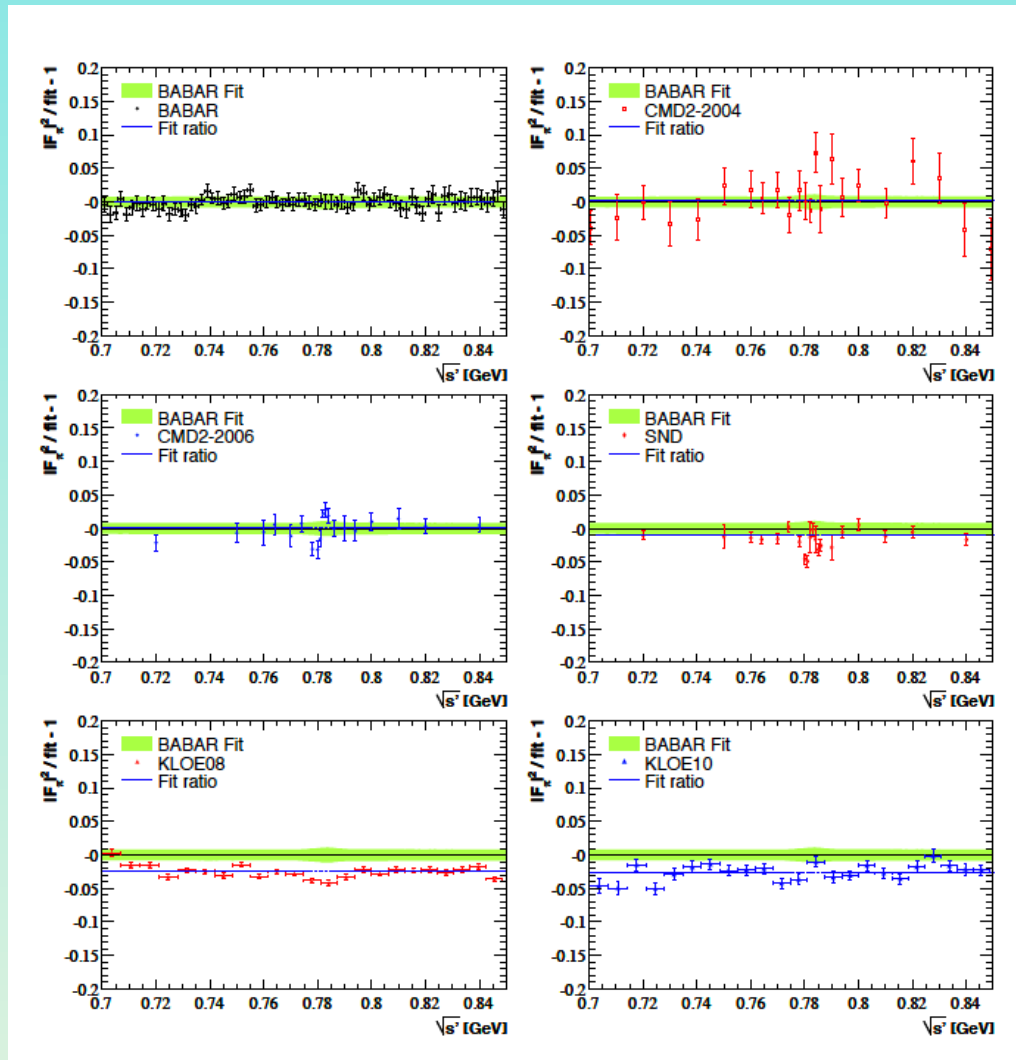
Sensitivity of $g - 2$ experiments to various contributions. The increase in precision with the BNL $g - 2$ experiment is shown as a cyan vertical band. New Physics is illustrated by the deviation $(a_\mu^{\text{exp}} - a_\mu^{\text{the}})/a_\mu^{\text{exp}}$

□ muon $g - 2$ very sensitive monitor to new physics. $3 - 4 \sigma$ deviation. Before LHC deviation seems to fit perfect with moderately light SUSY particle. LHC: $M_{\text{SUSY}} > 600 \text{ GeV}$ now requires very large $\tan\beta$ while $b \rightarrow s\gamma$ requires rather low $\tan\beta$!

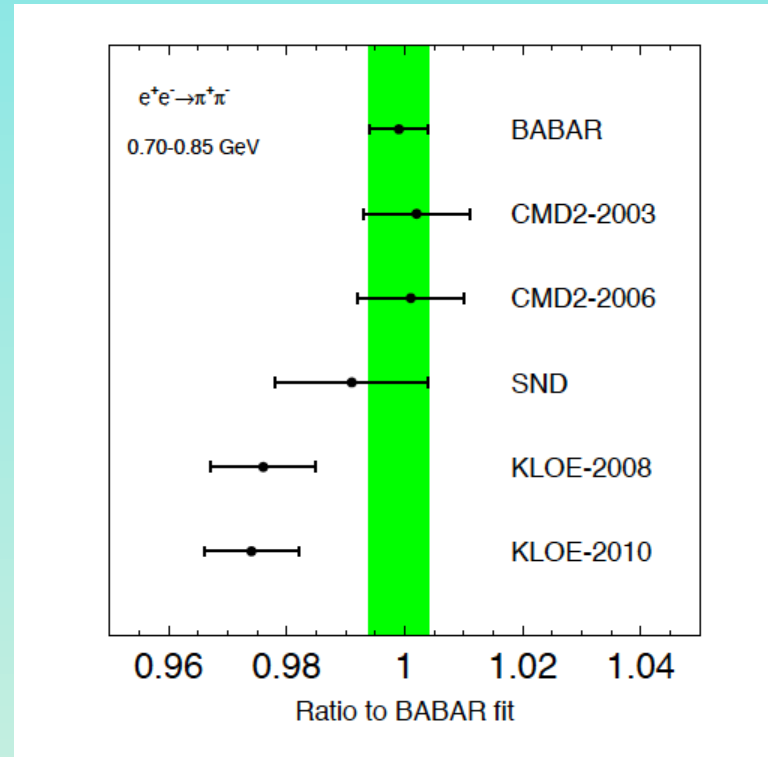
So what do we see in the muon $g - 2$???

You may find what it is!

Thank you for your attention!



Davier&Malaescu Reply



Davier&Malaescu Reply

g (HLS)	a (HLS)	$(c_3 + c_4)/2$	$c_1 - c_2$	v
5.578 ± 0.001	2.398 ± 0.001	0.920 ± 0.004	1.226 ± 0.026	0.030 ± 0.012
z_A	z_V	z_T	ϵ_0	—
1.608 ± 0.006	1.319 ± 0.001	1.409 ± 0.062	0.026 ± 0.003	—
Δ_A	Σ_A	Δ_V	Σ_V	h_V
0.048 ± 0.007	0	-0.028 ± 0.003	-0.034 ± 0.001	2.853 ± 0.291

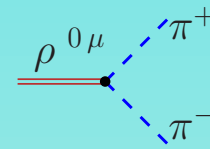
Parameter values from the global fit using the CMD–2, SND and KLOE10 data. The piece of information written boldface was not allowed to vary within the fit procedure.

Parameter	Sub. Pol. $\Pi_{\pi\pi}^{\rho}(s)$	Sub. Pol. $\Pi_{\pi\pi}^{W/\gamma}(s)$
C_1 (GeV ⁻²)	0	0.671 ± 0.041
C_2	-0.473 ± 0.001	0.730 ± 0.063
	Sub. Pol. $\varepsilon_2(s)$	Sub. Pol. $\varepsilon_1(s)$
C_1 (GeV ⁻²)	-0.075 ± 0.006	-0.015 ± 0.002
C_2	0.034 ± 0.005	0.015 ± 0.002

Parameter values from the global fit using the CMD-2, SND and KLOE10 data (cont'd). The boldface parameter is not allowed to vary. Each subtraction polynomial is supposed to be written in the form $C_1 s + C_2 s^2$. The functions $\varepsilon_1(s)$ and $\varepsilon_2(s)$ are combinations of the kaon loops which govern the neutral vector meson mixing.

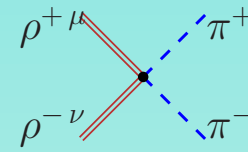
$g_{\rho\pi\pi}$	f_K/f_π	$g_{\omega\rightarrow\pi\pi}^{direct}$	λ
6.505 ± 0.003	1.279 ± 0.010	0.408 ± 0.061	$(7.64 \pm 3.19) 10^{-2}$
ϵ	ϵ'	θ_8 (deg)	θ_{PS} (deg)
$(4.027 \pm 0.474) 10^{-2}$	$(0.975 \pm 0.122) 10^{-2}$	$(-24.61 \pm 0.21)^\circ$	$(-13.54 \pm 0.15)^\circ$
m_ω (MeV)	Γ_ω (MeV)	m_ϕ (MeV)	Γ_ϕ (MeV)
782.52 ± 0.03	8.66 ± 0.04	1019.25 ± 0.26	4.18 ± 0.02
m_ρ (MeV)	Γ_ρ (MeV)	$\mathcal{R}e(s_\rho)$ (GeV ²)	$\mathcal{I}m(s_\rho)$ (GeV ²)
753.8 ± 0.5	138.10 ± 0.5	0.5682 ± 0.0007	0.1041 ± 0.0004

Physics parameters extracted from the BHLS favored fit.



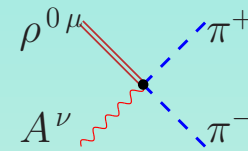
A Feynman diagram showing a rho meson (represented by two parallel red lines) entering from the left and splitting into two pions (represented by dashed blue lines) exiting to the right. The rho meson is labeled $\rho^{0\mu}$ and the pions are labeled π^+ and π^- .

$$:= -i g_{\rho\pi\pi} (p_- - p_+)^{\mu}$$



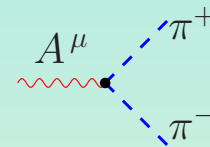
A Feynman diagram showing two rho mesons (represented by two parallel red lines) entering from the left and two pions (represented by dashed blue lines) exiting to the right. The rho mesons are labeled $\rho^{+\mu}$ and $\rho^{-\nu}$, and the pions are labeled π^+ and π^- .

$$:= 2i g_{\rho\pi\pi}^2 g^{\mu\nu}$$



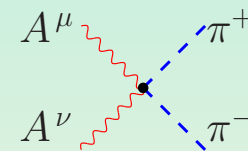
A Feynman diagram showing a rho meson (represented by two parallel red lines) and a photon (represented by a wavy red line) entering from the left and two pions (represented by dashed blue lines) exiting to the right. The rho meson is labeled $\rho^{0\mu}$ and the photon is labeled A^{ν} . The pions are labeled π^+ and π^- .

$$:= 2ie g_{\rho\pi\pi} g^{\mu\nu}$$



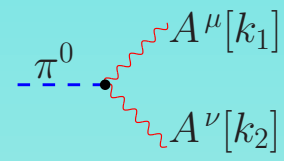
A Feynman diagram showing a photon (represented by a wavy red line) entering from the left and two pions (represented by dashed blue lines) exiting to the right. The photon is labeled A^{μ} and the pions are labeled π^+ and π^- .

$$:= -ie (p_- - p_+)^{\mu}$$

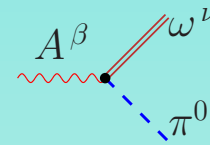


A Feynman diagram showing two photons (represented by wavy red lines) entering from the left and two pions (represented by dashed blue lines) exiting to the right. The photons are labeled A^{μ} and A^{ν} , and the pions are labeled π^+ and π^- .

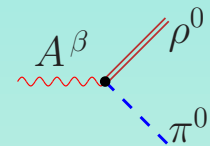
$$:= 2ie^2 g^{\mu\nu}$$



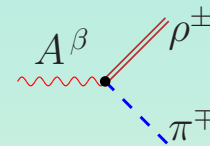
$$:= e^2 g_{\pi\gamma\gamma} \varepsilon^{\mu\nu\alpha\beta} k_{1\alpha} k_{2\beta}$$



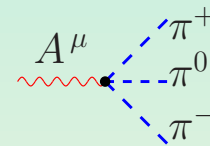
$$:= -i e g_{\omega\gamma\pi} \varepsilon^{\mu\nu\alpha\beta} p_{\gamma\alpha} p_{\omega\mu}$$



$$:= -i e g_{\rho^0\gamma\pi^0} \varepsilon^{\mu\nu\alpha\beta} p_{\gamma\alpha} p_{\rho\mu}$$



$$:= -i e g_{\rho^\pm\gamma\pi^\mp} \varepsilon^{\mu\nu\alpha\beta} p_{\gamma\alpha} p_{\rho\mu}$$



$$:= -e g_{\gamma\pi\pi\pi} \varepsilon^{\mu\nu\alpha\beta} p_{0\nu} p_{+\alpha} p_{-\beta}$$

$$\begin{array}{c} \omega^\mu \\ \hline \bullet \\ \begin{array}{l} \nearrow \rho^{0\nu} \\ \searrow \pi^0 \end{array} \end{array} := g_{\omega\rho\pi} \varepsilon^{\mu\nu\alpha\beta} p_{\omega\alpha} p_{\rho\beta}$$

$$\begin{array}{c} \omega^\mu \\ \hline \bullet \\ \begin{array}{l} \nearrow \rho^{\pm\nu} \\ \searrow \pi^\mp \end{array} \end{array} := g_{\omega\rho\pi} \varepsilon^{\mu\nu\alpha\beta} p_{\omega\alpha} p_{\rho\beta}$$

$$\begin{array}{c} \omega^\mu \\ \hline \bullet \\ \begin{array}{l} \nearrow \pi^+ \\ \rightarrow \pi^0 \\ \searrow \pi^- \end{array} \end{array} := -g_{\omega\pi\pi\pi} \varepsilon^{\mu\nu\alpha\beta} p_{0\nu} p_{+\alpha} p_{-\beta}$$

$$\begin{aligned}
 g_{\pi\gamma\gamma} &= -\frac{N_c}{24\pi^2 F_\pi} (1 - c_4) \\
 g_{\gamma\pi\pi\pi} &= -\frac{N_c}{12\pi^2 F_\pi^3} \left[1 - \frac{3}{4} (c_1 - c_2 + c_4) \right] \\
 g_{\omega\pi\pi\pi} &= -\frac{3N_c g}{16\pi^2 F_\pi^3} (c_1 - c_2 - c_3) \\
 g_{\pi\pi\pi\gamma} &= \frac{1}{4} \left(1 - \frac{1}{2} \Delta_A \right) \\
 g_{\omega\gamma\pi} &= -\frac{n_c g}{16\pi^2 f_\pi} (c_4 - c_3)
 \end{aligned}$$